International Journal of Applied Earth Observation and Geoinformation 144 (2025) 104850

Contents lists available at ScienceDirect

International Journal of Applied Earth Observation and Geoinformation

journal homepage: www.elsevier.com/locate/jag

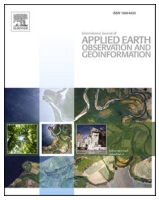

Mapping cervid forage in Sweden using remote sensing and national forest inventory data

Lukas Graf [a,*], Inka Bohlin [b], Per-Ola Hedwall [a], Jonas Dahlgren [b], Annika M. Felton [a]

[a] Swedish University of Agricultural Sciences, Southern Swedish Forest Research Centre, Box 190, SE- 234 22 Lomma, Sweden
[b] Swedish University of Agricultural Sciences, Department of Forest Resource Management, Skogsmarksgränd SE-901 83 Umeå, Sweden

ARTICLE INFO

Keywords:
Cervid forage mapping
Remote sensing
National Forest Inventory (NFI)
Wildlife management
Forest ecology

ABSTRACT

Cervid browsing influences forest ecosystems worldwide, stressing the need for wildlife management founded in accurate estimates of available forage. In this study, we developed the first national-scale models for Sweden to estimate the abundance of cervid forage by combining data from the National Forest Inventory (NFI) and different remote sensing (RS) datasets. We focused on six key forage tree species for cervids in Sweden: Scots pine (*Pinus sylvestris*), birch (*Betula* spp.), European aspen (*Populus tremula*), rowan (*Sorbus aucuparia*), oak (*Quercus* spp.), and goat willow (*Salix caprea*).

We combined airborne laser scanning and other auxiliary RS data with NFI data from 2016 to 2022 to model small tree abundance from 19 461 plots across Sweden in an area-based approach. We fitted generalized linear mixed models using likelihood-ratio tests to predict species-specific forage availability. Models were validated using an independent dataset of NFI data collected in 2023. Our models demonstrated moderate to strong predictive performance, with marginal R^2 values ranging from 0.226 to 0.973. Model validation suggested higher RMSE and rRMSE values for tree species that are scarce throughout the country than for more abundant species.

We provide maps for all six modelled tree species, both at a 1 ha and a 1 km^2 spatial scale, with the aim for them to be used in wildlife management, forestry planning, and ecological research. Our map products can for example help stakeholders assess a region's spatial distribution of cervid forage and thus inform habitat management and potentially mitigate browsing-related economic losses in forestry.

1. Introduction

Worldwide, members of the deer family (*Cervidae*) are influencing ecosystems and ecosystem processes through consumption of plant biomass (Apollonio et al., 2017; Forbes et al., 2019). In many parts of the world, the influence of cervid species on vegetation has grown due to increasing population densities over the past century (Apollonio et al., 2017; Côté et al., 2004). In forest ecosystems, cervids may limit reproduction and growth rates of young trees through browsing (De Vriendt et al., 2023; De Vriendt et al., 2021). In production forests, damage induced by cervids can reduce wood quality and induce long-term changes in canopy structure, for example through bark stripping or top shoot browsing (Gill, 1992; Widén et al., 2022), thereby affecting the timber production (Cukor et al., 2019). Due to the major impacts cervids can have on forest ecosystem services (i.e., timber production or carbon sequestration), forestry often requires management of cervid populations (Apollonio et al., 2010). The amount of browsing damage however may depend on other factors in addition to their population density, such as the amount of locally available forage (Felton et al., 2022; Widén et al., 2024), silvicultural practices (Domisch et al., 2024), as well as forest and landscape composition (Nikula et al., 2021).

In the boreal biome, cervid diets are often composed of small trees, shrubs and herbs (Spitzer, 2019). In Scandinavia for example, moose (*Alces alces*) and other cervids feed on the common species Scots pine (*Pinus sylvestris*) and birch (*Betula* spp.), as well as the preferred, but rarer European aspen (*Populus tremula*), rowan (*Sorbus aucuparia*), oak (*Quercus* spp.), goat willow (*Salix caprea*), from here on abbreviated AROW. It is the cervids' browsing on the top shoots of young Scots pine that causes the largest economic loss for Scandinavian forestry (Wam and Hofstad, 2007). Moose cause the majority of this damage, and a conclusion in many studies is that the amount of damage in Scots pine plantations is influenced by the availability of Scots pine and other forage plants, in addition to the density of the local moose population (Felton et al., 2022; Herfindal et al., 2015; Månsson, 2009). Despite this

* Corresponding author.
E-mail address: lukas.graf@slu.se (L. Graf).

https://doi.org/10.1016/j.jag.2025.104850
Received 9 April 2025; Received in revised form 10 September 2025; Accepted 11 September 2025
Available online 18 September 2025

knowledge, large-scale estimates of the availability of forage plant species are scarce. Instead, management decisions are based upon a coarse measure of alternative forage, in Sweden namely the area of young forest estimated to be within browsing height (Swedish Forest Agency, 2024). This successional stage of the forest has the highest concentration of trees within browsing height of moose (Bergqvist et al., 2018; Wam et al., 2010). However, this areal measure lacks fine-scaled information on tree species composition and abundance, which is crucial for predicting browsing damage. For example, damage on Scots pine is negatively related to abundance of AROW at the landscape level (Felton et al., 2022), making specific estimates of these tree species disproportionately valuable for forest planning and wildlife management. Additionally, about 50 % of the tree forage ingested by moose is consumed in older forests (Bergqvist et al., 2018), stressing the need for complementary datasets on available forage (Apollonio et al., 2017).

Efficient wildlife and forest management requires precise estimates of available forage, and the development of remote sensing (RS) based forest maps (Mensah et al., 2023; Nilsson et al. 2017) facilitates opportunities for management to obtain these across large landscapes (Borowik et al., 2013; Lone et al., 2014). Field data from large scale campaigns such as the Swedish National Forest Inventory (NFI) data can be successfully combined with different remote sensing sources, e.g. satellite images and airborne laser scanning (ALS), to link forest attributes measured to various remote sensing metrics for national prediction models (Bohlin et al., 2017; Herfindal et al., 2015; Nilsson et al., 2017). Although not often used to map understory, low density ALS data appears to be a promising data source to model cervid forage within browsing height (here: 0.5–4 m), as it allows to derive metrics (Bohlin et al., 2021; Maltamo et al., 2014; Melin et al., 2016a) that approximate forest structure and have been used to model understory vegetation (Barber et al., 2016; Lucas et al., 2010; Nijland et al., 2014). In Sweden, many ALS based map products for the forest sector are currently developed yet maps with detailed information on forage availability or understory composition are missing. The ALS data collected in Sweden

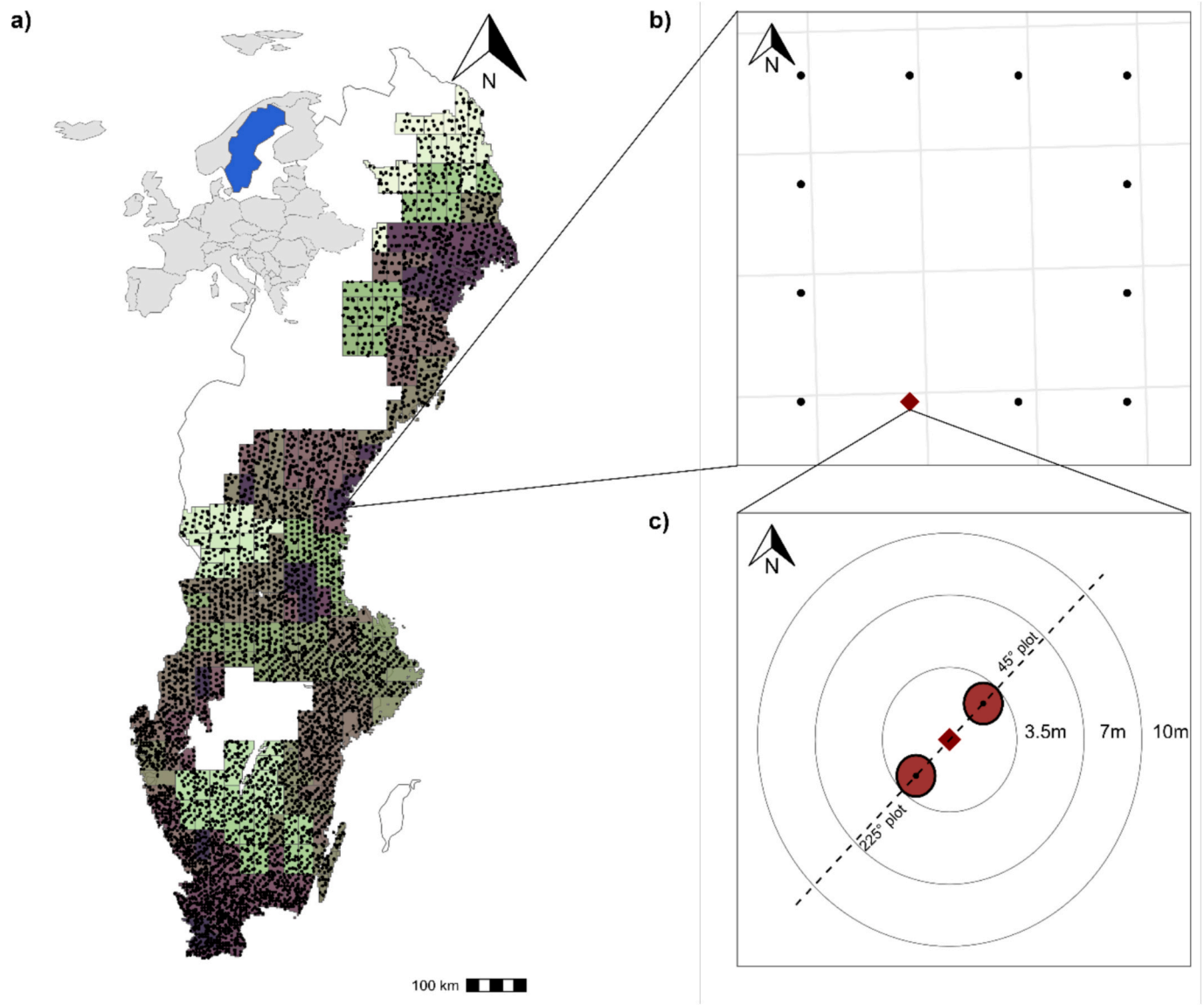

Fig. 1. Overview on the data collection design in this study. a) The location of Sweden on the inset Europe map and the distribution of the clusters of the NFI in Sweden (black points). The colored squares in the background delineate the scanning blocks of the second Swedish Laser Scanning Survey used in this study. b) An example of an NFI cluster. The sizes of the clusters vary between regions in Sweden and the length of the cluster sides increase towards the north from 300 m to 1800 m. c) the individual plot design of NFI. The red square indicates the center of the plot, the two red circles (located at 45° and 225° from the center) indicate the 1 m radius subplots (3.14 m^2 per plot) in which our response variable has been measured. We also show the 3.5 m, 7 m (temporary) and 10 m (permanent) radii in which the NFI collects further variables. (For interpretation of the references to colour in this figure legend, the reader is referred to the web version of this article.)

are used to create, for example, the national forest attribute map (Nilsson et al., 2017), the soil moisture map (Ågren et al., 2021) or to map site indices (Mensah et al., 2023), while the National land use map and tree species maps are combining ALS and Sentinel 2 satellite images (SLU Skogsdata, 2019; Swedish Land Survey, 2020).

In this study we developed the first national models for Sweden to estimate the availability of forage trees (as the abundance of Scots pine, birch and AROW) within browsing height, by using data from the NFI in combination with wall-to-wall RS based auxiliary data. Finally, we provide species-specific maps of cervid forage and discuss the potential application of the underlying models in forest and cervid management as well as in further research.

2. Methods

2.1. The Swedish national forest inventory

The Swedish NFI has collected nation-wide data (Fig. 1a) on the state of the forest for over 100 years (Fridman et al., 2014; Tomppo et al., 2010). Within this monitoring program, data are collected on forest attributes such as standing tree volume and tree species composition, as well as composition of the shrub layer and amount of tree regeneration (SLU Riksinventering, 2023). Data are collected in circular sampling plots from May until October, that are either permanent (r = 10 m) or temporary (r = 7 m) and a GPS position with float-level accuracy of the center of the plot is recorded (SLU Riksinventering, 2023). The permanent plots are re-inventoried every fifth year, while the temporary plots are inventoried only once. The NFI plots are nested in clusters of several plots (Fig. 1b). The sampling intensity decreases towards the north with increasing distances between clusters and between plots in the clusters.

In this study we used Swedish NFI data from 2016 to 2022 on both temporary and permanent plots on productive forest land, corresponding to the collection years of ALS data (see below) to model the abundance of small trees that are available for browsing by large ungulates. Productive forest land is defined by a capacity for stem wood production >1 m^3 $year^{-1}$ ha^{-1}. In two 3.14 m^2 subplots (r = 1 m) per main plot (Fig. 1c), the NFI counts the number of small trees with a minimum height of 10 cm and a maximal diameter at breast height of 4 cm. We expected this to reflect the browsing height window, i.e. the height window in which most of browsing occurs, which normally is defined as trees between 0.5 and 4 m. The two 3.14 m^2 subplots are placed 2.5 m from the center of each main NFI plot, at a 45- and 225-degree placement (Fig. 1c). We only used data from non-divided NFI plots, i.e. where the whole plot fell in a single forest stand. In total, we used data from 19,461 NFI plots. The mean number of small trees per main plot was highest for birch (mean = 0.912, SD = 3.15, n_{total} = 21135), followed by pine (mean = 0.516, SD = 1.81, n_{total} = 11965), rowan (mean = 0.351, SD = 1.28, n_{total} = 8136), aspen (mean = 0.174, SD = 1.13, n_{total} = 4032), oak (mean = 0.070, SD = 0.712, n_{total} = 1615) and willow (mean = 0.056, SD = 0.487, n_{total} = 1299, Fig. A1). Pine, birch, rowan and aspen are common throughout the country, while oak is mostly concentrated in the southern parts of Sweden. Willow abundance is low throughout the country. We used the sum of small trees recorded in the two subplots (small trees per 6.28 m^2) for the six different species (AROW, pine and birch) as our response variables in the modelling process.

2.2. Remote sensing data and predictor variables

2.2.1. ALS data

ALS data used in this study was collected from 2018 to 2022, using with the ALS80-HP, City Mapper, City Mapper 2 and Terrain Mapper ALS scanners by the second Swedish Laser Scanning Survey (SLSS) in 25x50 km laser blocks (Fig. 1a). At the end of 2022, the SLSS covered about 70.4 % of the country. Flight heights were at approximately 3000 m, scanning angles were at a maximum of ± 20°. Point densities in the data were 1.392 ± 0.513 points per m^2 (Lantmäteriet, 2022), with a positional accuracy a standard error of 0.1 m in height and 0.3 m in the plane (Lantmäteriet, 2022). The national digital elevation model (DEM) was used as a reference when normalizing the above ground heights of ALS returns (Lantmäteriet, 2020). Points have been classified into ground, water, bridge, low point (noise) and high noise (e.g., cloud), as well as an unclassified class. As we only use data from plots that fell onto forested land, we did not further filter ALS point clouds based on these criteria but based on NFI data and landuse classes. ALS returns above 40 m are excluded in this dataset, as they likely refer to outliers such as clouds or birds. Phenological mismatches due to seasonality between acquisition of ALS data and NFI data were largely neglectable, as the NFI data is only collected in the summer throughout the entire country and the number of trees can be assessed without consideration of seasonality.

Using low density ALS data prohibited us from directly measuring the abundance of forage (in terms of trees per plot) on the plot level, especially in older forests with dense canopy cover it is impossible to detect small trees using low density ALS data. Instead, we aimed to use an area-based approach to indirectly model the abundance of trees, i.e. derive information on forest structure from the ALS point clouds and link it to abundance of small trees. Therefore, we calculated point cloud metrics describing canopy cover, small tree cover and canopy height for each plot. Although up to seven returns were theoretically available (Lantmäteriet 2022), we decided to use first returns only, to obtain more robust estimates for height values and more consistent values across all plots and scanning blocks. We considered these variables to reflect forest structure (together with information regarding the main tree species present, from other Swedish mapping products), and therefore serve as predictors of young trees within browsing height, based on previous studies (Barber et al., 2016; Bohlin et al., 2021; Lucas et al., 2010; Melin et al., 2016a).

We first calculated canopy cover as the percentage of the ground covered by the tree canopy (see Eq. (1)).

$$\frac{n_{firstreturnsabove5m}}{n_{allfirstreturns}} * 100 \quad (1)$$

Next, we calculated the cover of potential small trees, which we called "small tree cover" (see Eq. (2)).

$$\left(\frac{\%_{all\ first\ returns\ below\ 4m}}{\%_{all\ first\ returns\ below\ 0.5m}}\right) \Big/ \%_{all\ first\ returns\ below\ 4m} * 100 \quad (2)$$

Canopy height in meters above ground was calculated as the 95 % quantile where all first returns were accumulated (commonly referred to as 95 % height quantile) (Bohlin et al., 2021; Melin et al., 2016b). In Sweden the SLSS scans forests during different phenological conditions of trees i.e. leaf-on (north of Sweden) and leaf-off (south of Sweden), which can affect the ALS point cloud characteristics, especially in deciduous and mixed forests. To take that into account we also created the metric leaf-on/leaf-off canopy cover (Imangholiloo et al., 2019), which we set to zero if the scanning was done during the leaf-off season (see section: *Land use data and tree species proportions* for definitions). If the ALS data was collected during the leaf-on period, this metric is equal to canopy cover. All ALS based point cloud metrics were calculated by clipping the point clouds to a 7 m buffer (corresponding to temporary plots) around the center of the NFI plots using the LidR-package (Roussel et al., 2020) using the *cloud_metrics*() – function. A detailed overview of all calculated predictor variables can be found in Table 1.

2.2.2. Climatic data

In Sweden, climate strongly influences forest structure and tree species distributions (Lenoir and Svenning, 2014; Walck et al., 2011), which motivated us to include bioclimatic variables into our dataset. We extracted two bioclimatic variables from datasets available from worldclim.org (Fick and Hijmans, 2017). We extracted mean annual

Table 1
Variables used in the modelling process with definitions, ranges, dataset source, and motivation for inclusion. The column range gives the range in the data, mean and one standard deviation around the mean. The range of and SD of the second order polynomials are in Table A2.

Variable	Definition	Range	Data source	Motivation
canopy height	Calculated as the 95 % quantile of first echoes	0–31.5 m (13.9 ± 6.23 m)	SLSS by National Land survey	Reflects stand development stage and light availability
canopy cover	Canopy cover as the proportion of echoes over 5 m from all first echoes	0–99.6 % (50 ± 27.4 %)		Affects understory light availability and degree of amensalism from larger trees
leaf on/leaf off canopy cover	Canopy cover with specification on scanning time	0–99.6 % (41.6 ± 31.3 %)		Accounts for structural differences between scanning dates (summer/spring/autumn)
small tree cover	Proportion of first echoes between 0.5 and 4 m	0–100 % (26.8 ± 19.7 %)		Reflects a direct ALS based structural metric for the response variable
annual mean temperature	Mean annual temperature at the plot	−2.17 °C–7.97 °C(3.80 ± 2.28 °C)	Worldclim.org	Temperature limits reproduction, survival and growth of plants
annual precipitation	Mean annual precipitation at the plot	436–1198 mm (676 ± 119.0 mm)		Precipitation limits reproduction, survival and growth of plants
land use class	Categorical with 4 classes	clear cut, deciduous forest, coniferous forest, mixed forest	Swedish Landcover Map	Provides information on the dominant vegetation
soil moisture	Soil moisture in %	0–100 % (32.9 ± 33.4 %)	SLU Soil Moisture Map	Soil moisture limits reproduction, survival and growth of plants
elevation	Height above sea level	0.4 m–812 m a.s.l. (217 ± 143 m)	SLSS by National Land survey	Elevation limits plant distribution due to larger variation in temperature
slope	Elevation change to surrounding pixels	0.3–42° (5.61 ± 4.7°)		Slope impacts light availability and soil conditions
deciduous/conifer proportion	Proportion of coniferous/deciduous volume from total estimated volume	0–100 % (18.9 ± 23 % deciduous proportion)/ (81.1 ± 23 % conifer proportion)	SLU species map	Tree species composition influences the effect of canopy cover on understory light availability and seed availability
Spruce proportion	Proportion of spruce from total estimated volume	0–100 % (34.8 ± 26.6 %)		
Second order polynomial terms				We included second order polynomial terms to account for non-linear responses to predictor variables
Two-way interactions				We included two-way interactions between land use classes as well as all ALS based data and their second order polynomials to account for non-linear gradients in our response variable in relation to the predictor
Final model				The final model formulations can be found in supplementary materials A

temperature, and the mean annual precipitation sum based on the years 1970 to 2000. Data from worldclim.org is available at a 1 km x 1 km spatial resolution. Data was extracted using 7 m-radius buffers around the center of the NFI plot. In case a plot fell into several raster cells, we calculated the mean values of the cells (Fick and Hijmans, 2017).

2.2.3. Terrain data

We extracted data from the ALS derived digital elevation model (DEM) (Lantmäteriet, 2020) for Sweden and SLU soil wetness (SW) map (Ågren et al., 2021), which is partially modelled using the DEM. Both have a 2x2m spatial resolution and have previously been used to model NFI data with ALS data (Bohlin et al., 2021). We extracted elevation from the DEM and soil wetness from the SW map using a 7 m radius buffer around the NFI plot and calculated mean elevation and SW of all raster cells intersecting the buffer. We further calculated the mean slope from the DEM inside the 7 m buffer.

2.2.4. Land use data and tree species proportions

Lastly, to account for the effect of forest type, we extracted data from the National Land Cover map using pointwise extractions (Swedish Land Survey, 2020), that we reclassified (see details on the reclassification in Table A1). We only included land-cover data that overlapped with NFI plots that fell on forested land or clear-cuts (defined as temporary non-forested areas). We also calculated the proportion of coniferous and deciduous tree species, as well as Norway spruce (*Picea abies*) proportions, by overlapping NFI plots using species specific volume maps with a 12.5 x 12.5 m spatial resolution (SLU Skogsdata, 2019). All proportions were calculated using the mean of all cells intersecting a 7 m buffer around the NFI plot.

2.2.5. Matching the NFI and remote sensing data

We included NFI plots that were inventoried within three years before or after ALS data collection (see Bohlin et al. (2021) for further details). Further, to remove outliers or NFI plots with mismatches between ALS data and field inventory data from the NFI (caused by time difference in data collection) and thus ensure high agreement between NFI and RS data, we used Mahalanobis distance to quantify how volume and tree height from laser based National forest attribute maps deviate from those measured in the field, taking into account the covariance structure of the dataset to ensure scale- and correlation-aware comparisons (Leys et al., 2018). Tree height and volume raster are based on the same laser data as our laser metrics. We removed all plots from further analysis that were outside the upper 95 % quantile of the calculated Mahalanobis distance. Further, we only used plots with a minimum mean point density of 1 point per m^2 to ensure that ALS based metrics had sufficient data to represent the forest characteristics during the scan. Our final dataset consisted of data from 19,461 NFI plots in 4736 clusters and 252 scanning blocks. Due to the small size of the small tree subplots (2 x 1 m radius circular plots) in relation to the pulse density of the ALS data, it is impossible to count the small trees directly using low density ALS data. Therefore, we applied an area-based approach as an indirect way to model the number of small trees based on the correlation between the RS data and the measured number of small trees from the NFI (see e.g. Bohlin et al. (2021) for a similar application of this approach).

2.3. Statistical analysis

2.3.1. Modelling small tree abundance

We applied generalized linear mixed effect models (GLMMs) with a negative binomial error distribution and log link-function, using the species-specific aggregated number of small trees in the two NFI subplots (number of small trees per 6.28 m^2) as the response variable and RS variables (Table 1) as predictor variables. We used the *glmmTMB()* function in the R package *glmmTMB* (Brooks et al., 2017). See Fig. A1 in Supplementary Materials A for species specific distributions of the

response variable. We fitted separate sets of models for each tree species. We chose the cluster of the NFI data as well as the laser scanning block as random intercepts to account for non-independence and hierarchy of the NFI data and the ALS data. Willow was observed in few plots and these plots were distributed among an almost equal number of clusters and scanning blocks which led to non-convergence and singularity issues in the GLMM structure described above. Instead, we fitted a generalized linear model (GLM) with a negative binomial distribution using the *MASS* package for willow (Ripley et al., 2013).

To account for non-linear relationships between our response variable and the underlying Gaussian process, we included first- and second-order polynomial terms of all numerical variables (Table 1) except leaf-on/leaf-off canopy cover into the modelling process. We included various two-way interactions between our predictor variables (e.g., canopy cover x canopy cover^2, canopy cover x canopy height and canopy cover x canopy height^2). We included interactions between landcover and all numerical covariates (e.g., land use x canopy height and land use x canopy height^2) and between second order polynomials (e.g., canopy cover^2 x spruce proportion^2). We used z-score transformation to bring variables to similar scales and ease model convergence. We z-score transformed first and second order polynomial terms separately to ensure independence between variables and prevent strong outliers in the scaled data.

We first identified a global, maximal model for each tree species that contained as many variables as possible while ensuring convergence. For deciduous tree species, we used coniferous proportion as a covariate, whereas we used deciduous proportion as a covariate for Scots pine. Next, we refitted the model with removed terms and used Likelihood-ratio tests to compare goodness of fit between models to stepwise reduce model complexity based on significant contribution of predictors and interactions to the model, using the *buildglmmTMB()* function in the *buildmer package (*Voeten, 2021*)* (see Supplementary Materials A for more information). This was done to avoid overfitting and ensure that the model only contains terms and interactions that are important to model the abundance of our target species. In the elimination phase of the terms, we fitted models using restricted maximum likelihood. After the best model had been found we refitted the model using maximum likelihood.

2.3.2. Model assessment and validation

We validated our models with a new data set from temporary NFI plots and SLSS collected in 2023 (Fig. A2). Based on the model predictions on this new data, we calculated root mean squared errors (RMSE) and relative RMSE (rRMSE) as metrics of model performance. As they are only inventoried once, we only used temporary plots for model validation. The validation dataset contained 1324 temporary NFI plots, and we applied the same temporal thresholds as for the training data (i.e. a maximal temporal mismatch of three years between data acquisition and NFI measurement; Fig. A2). Further, to assess overall model fit, we calculated Nakagawas R^2 (Nakagawa et al., 2017) and Nagelkerkes R^2 (willow only) (Nagelkerke, 1991) using the *performance* package (version 0.10.6) (Lüdecke et al., 2021). As we found strong effects of the climatic variables on oak abundance, we further refitted the final oak model without these to estimate the importance of the other, non-climatic, variables.

2.3.3. Mapping and spatial uncertainty

Prediction of forage availability map products was done for 10x10m (the same spatial grain of the training unit) grids over whole Sweden, which corresponds to the size of the NFI plots. We applied the *predict*() function of the *glmmTMB* and *MASS* packages and predicted the mean estimate. We accounted for spatial autocorrelation of the prediction error during aggregation by following section 4.1 of Wadoux and Heuvelink (2023) and showcased this in one moose management area by further predicting the standard error estimated by the models on the maps. We then fitted variograms with a spherical function to the residual error of the validation dataset using the *gstat* package (Pebesma, 2004). We accounted for spatial autocorrelation of the predicted standard errors by applying Formula 7 in Wadoux and Heuvelink (2023) to calculate the average aggregated standard error, using 100 random samples per hectare (the maximum amount of cells available per hectare) and calculated the upper and lower 95 % confidence limits of the predictions. The map products are presented as aggregated versions of 1 ha grids for moose management areas, and 1 km^2 grids for the whole nation. For more details on map demonstration see Supplementary Materials A, section "Mapping and model demonstration" and Fig. A3. All statistical analysis was conducted in R version 4.4.1 (R Core Team, 2024).

3. Results

3.1. Best models for small tree abundance

The best models after model selection had a marginal (fixed effects only) R^2 ranging from 0.226 to 0.973 and a conditional (full model, including random effects) R^2 ranging from 0.432 to 0.979 (Table 2). Pine abundance was strongly related to metrics derived from ALS data, namely small tree cover, canopy cover and their second order polynomials, and interactions between these (Fig. A4, Supplementary Materials B Table B1). Birch abundance was strongly related to canopy height, canopy cover and interactions between the first and second order polynomials of them (Fig. A5, Table B2). We found strong effects of mean annual temperature on oak abundance (Fig. A6, Table B3), but also of canopy height, canopy cover and land use class. The refitted oak model without an annual mean temperature had a conditional R^2 = 0.872 and a marginal R^2 = 0.053, suggesting that a large amount of variation in oak abundance is explained by climatic variables. The abundance of willow was strongly linked to canopy cover, and to conifer proportion, as well as their first and second order polynomials (Fig. A7, Table B4). Likewise, rowan abundance showed a strong correlation with canopy cover, canopy height as well as interactions with conifer proportion, canopy height and cover (Fig. A8, Table B5). Abundance of aspen was influenced by land use class, canopy cover and height, as well as interactions between land use class and canopy cover, and between land use class and canopy height (Fig. A9, Table B6). Table 2 shows the overview of rRMSE and R^2 for all models.

Fig. 2a–f shows the spatial predictions to illustrate the differing distributions of small trees of our six target species across Sweden at a 1 km^2 resolution, while Fig. 3 a-f shows the same spatial predictions in a specific MMA, but aggregated to a 1 ha spatial resolution. We further provide upper and lower 95 % confidence intervals in model predictions for the aggregated map products for Fig. 3. Note for example the clear geographical trend in Fig. 2c for oak as well as the tendency for subtle south-north gradients in Figs. 2d and f for pine and willow.

Table 2
Overview on conditional and marginal Nakagawa R^2 of the final GLMMs to predict the abundance of aspen, birch, oak, pine, rowan and willow, as well as root mean squared error (RMSE) and relative RMSE (rRMSE) for the predicted amount of small trees per plot (6.28 m^2) on the independent test dataset of the National Forest Inventory (NFI) from 2023. For willow, we fit a GLM and report Nagelkerkes R^2 (marked with an *) instead.

Species	Conditional R^2	Marginal R^2	$RMSE_{test}$	$rRMSE_{test}$
Aspen	0.515	0.317	1.228	7.818
Birch	0.550	0.421	2.395	3.280
Oak	0.979	0.973	0.325	6.337
Pine	0.630	0.481	1.391	3.174
Rowan	0.432	0.247	1.034	3.516
Willow	–	0.226*	0.371	11.983

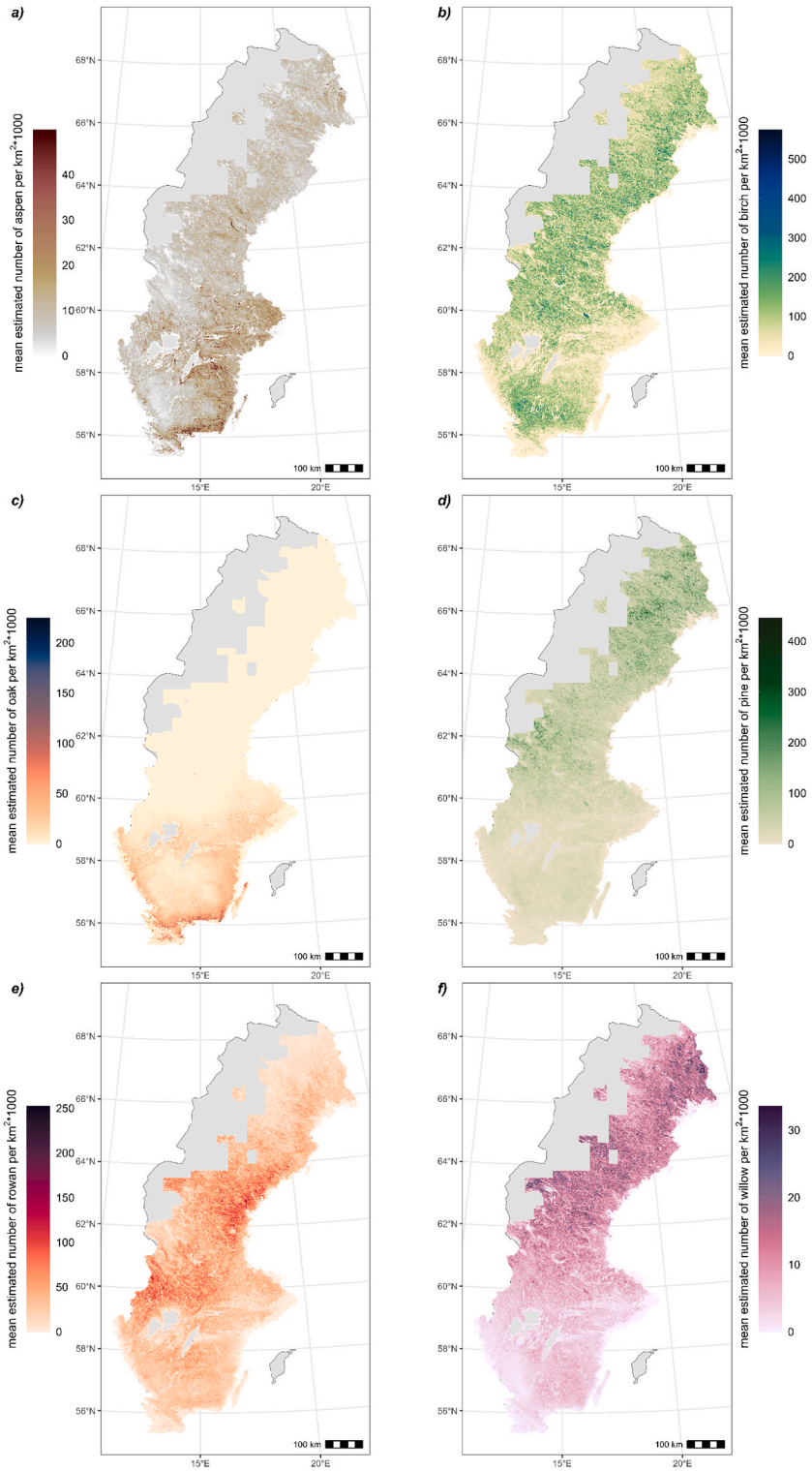

Fig. 2. Predicted abundance of the final models of six tree species (aspen (Populus tremula) (a), birch (*Betulus* spp.) (b), oak (*Quercus* spp.) (c), pine (*Pinus sylvestris*) (d), rowan (*Sorbus aucuparia*) (e) and goat willow (*Salix caprea*) (f)) across Sweden at a 1 km^2 spatial resolution. Grey areas indicate parts with missing ALS data from the SLSS. The extent of the predictions differs between this figure and the extent of the ALS – scanning blocks in Fig. 1a), as we added the data collected by the SLSS in 2023 into the prediction besides the SLSS data that were used to build the models. We calculated the mean estimated number of small trees per km^2 (trees within the NFI subplots from 0.1 m height to 4 cm diameter at breast height) by aggregating the cells to a 1 km^2 spatial resolution and upscaling the predicted number of trees from plot level (6.28 m^2) to 1 km^2 by multiplying the mean predicted number of trees by 1 km^2/6.28 m^2. Note the difference in scale among the six tree species.

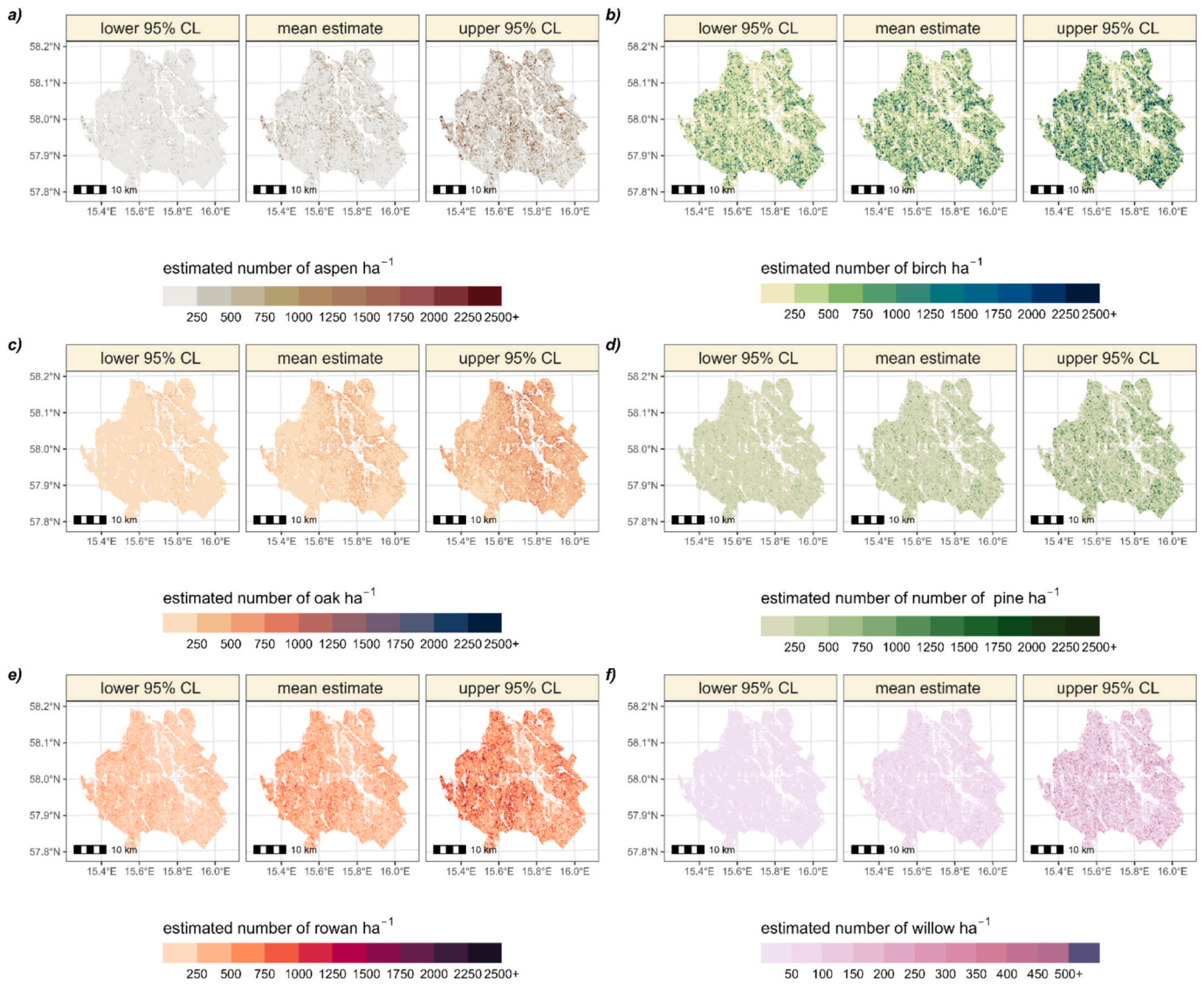

Fig. 3. Lower 95 % Confidence Limits (CL), mean estimates, and upper 95 % CL for the six tree species (aspen (*Populus tremula*) (a), birch (*Betulus* spp.) (b), oak (*Quercus* spp.) (c), pine (*Pinus sylvestris*) (d), rowan (*Sorbus aucuparia*) (e) and goat willow (*Salix caprea*) (f)) at a 1 ha spatial resolution in the Moose Management Area (MMA) Kinda Östergötland 5. This specific MMA is 129.104 ha in size. We calculated the mean estimated number of small trees per 1 ha by aggregating the cells from a 10x10m spatial resolution to a 100x100m spatial resolution and upscaling the predicted number of trees from plot level (6.28 m^2) to 1 ha by multiplying the mean predicted number of trees by 1 ha/6.28 m^2. We calculated the upper and lower 95 % CL by following Wadeux and Heuvelink (2023).

3.2. Model accuracy and performance

Model validation using independent data collected by the NFI in 2023 showed that RMSE was lowest for willow, oak and rowan (Table 2). rRMSE however was highest for willow, aspen and oak, the least abundant tree species in the dataset. Models tended to underestimate large amounts of trees but were moderately accurate in predicting small amounts of small trees (Table A3).

Residual prediction error varied by species and height class, canopy cover class and small tree cover class (binned, in incremental 25 % groups, see Table 3). In the lowest ALS based height class (0–5 m), most species showed negative residual error, indicating underestimation, with the exception of pine, which had a consistent positive residual error. Birch showed the strongest underestimation at this height. As canopy height increased, residual error generally became smaller in magnitude, with many species showing near-zero bias in the 10–15 m and +15 m ALS based height classes. Pine maintained a consistent positive bias across all height classes, while oak showed minimal bias throughout. These trends suggest that model accuracy improved with increasing canopy height.

At low canopy cover (0–25 %), most species exhibited a slight negative residual error, with birch showing the strongest negative bias. Pine consistently had a positive mean error across all cover classes, indicating a tendency for overestimation. As canopy cover increased, mean errors for most species moved closer to zero, suggesting improved model performance. Oak displayed minimal bias across all cover classes, while birch showed a decrease in residual error the higher canopy cover became. Overall, residual error was smallest at the highest canopy cover class (75–100 %), indicating better model accuracy with higher canopy cover.

For aspen and birch, the residual error showed a negative trend with increasing small tree cover, indicating underestimation in denser understories. In contrast, oak exhibited minimal and relatively stable mean errors across all classes, suggesting consistent model performance. Pine consistently showed positive residual error up to 50–75 % small tree cover, shifting slightly negative at the highest class (75–100 %). Rowan showed a mixed pattern, while willow had modest but consistently negative errors that became slightly more pronounced at higher small

Table 3
Overview on mean residual prediction error (small trees per 6.28 m^2 subplot of the NFI data) by the Airborne Laser Scanning (ALS) based canopy height class (in 5 m increments), canopy cover (in 25 % increments) and small tree cover (in 25 % increments) of the validation dataset of the NFI collected in 2023, which contained information on the number of small trees per 6.28 m^2 on an independent set of plots. We provide, for each group, the mean residual error (mean) as well as one standard deviation (SD) of the residual error after prediction.

	Canopy height			Canopy cover			Small tree cover		
Species	class	mean	SD	class	mean	SD	class	mean	SD
Aspen	0–5 m	−0.084	1.448	0–25 %	−0.081	1.138	0–25 %	−0.057	1.307
	5–10 m	−0.004	0.570	25–50 %	−0.006	0.989	25–50 %	0.033	1.156
	10–15 m	−0.010	0.709	50–75 %	−0.003	1.782	50–75 %	−0.005	1.173
	+15 m	−0.038	1.531	75–100 %	−0.032	0.373	75–100 %	−0.218	0.727
Birch	0–5 m	−0.107	4.682	0–25 %	−0.277	3.849	0–25 %	0.055	2.552
	5–10 m	−0.480	2.110	25–50 %	−0.296	1.232	25–50 %	−0.140	2.174
	10–15 m	−0.059	1.757	50–75 %	0.086	1.914	50–75 %	−0.413	2.183
	+15 m	0.044	1.577	75–100 %	0.069	1.110	75–100 %	−0.631	2.147
Oak	0–5 m	−0.005	0.279	0–25 %	−0.010	0.238	0–25 %	0.003	0.303
	5–10 m	−0.006	0.178	25–50 %	0.039	0.495	25–50 %	−0.001	0.281
	10–15 m	0.019	0.425	50–75 %	−0.001	0.303	50–75 %	0.033	0.541
	+15 m	0.001	0.311	75–100 %	>0.001	0.278	75–100 %	−0.020	0.056
Pine	0–5 m	0.204	1.765	0–25 %	0.201	2.194	0–25 %	0.108	1.370
	5–10 m	0.112	1.955	25–50 %	0.204	1.534	25–50 %	0.128	1.567
	10–15 m	0.149	1.237	50–75 %	0.036	0.733	50–75 %	0.080	1.204
	+15 m	0.043	1.055	75–100 %	0.012	0.327	75–100 %	−0.025	0.559
Rowan	0–5 m	−0.044	0.867	0–25 %	0.018	0.965	0–25 %	0.033	0.930
	5–10 m	0.134	1.091	25–50 %	0.113	0.994	25–50 %	−0.035	0.802
	10–15 m	−0.005	0.591	50–75 %	−0.008	1.211	50–75 %	0.076	1.893
	+15 m	−0.004	1.251	75–100 %	−0.046	0.898	75–100 %	−0.098	0.461
Willow	0–5 m	−0.078	0.294	0–25 %	−0.066	0.273	0–25 %	−0.021	0.201
	5–10 m	−0.086	0.258	25–50 %	−0.052	0.221	25–50 %	−0.014	0.591
	10–15 m	−0.059	0.117	50–75 %	−0.026	0.215	50–75 %	−0.098	0.276
	+15 m	0.017	0.498	75–100 %	0.010	0.611	75–100 %	−0.123	0.246

tree cover. Overall, model accuracy declined with increasing small tree cover for most species, particularly birch and aspen.

Lastly, the histograms presented in Fig. 4 show how presence and absence of small trees are related to common ALS based variables (canopy height, canopy cover and small tree cover), indicating the variability in tree abundance in relation to these metrics. Especially for canopy height and canopy cover, these differences in the distributions were visible, highlighting the importance of including these datasets into the models.

4. Discussion

4.1. Modelling small vegetation as forage abundance with NFI data and remote sensing

In this study, we combined NFI data and several wall-to-wall remote sensing-based datasets to model the abundance of tree species important as cervid forage. To our knowledge, studies focusing on the abundance of small trees within a small height window are scarce. The models we created enabled us to produce nationwide and region-specific forage abundance maps for these species (Figs. 2-3), with the aim to use them in future research and wildlife management in Sweden. Most of the previous studies combining large NFI datasets with RS data have predicted traditional forest variables, such as volume and tree height of dominant tree layer, above ground biomass, or tree species (e.g. Bohlin et al. (2017) and Nilsson et al. (2017)), whereas the shrub – and small tree layer has been largely neglected in these studies. Additionally, often young forests are excluded in these applications because of low prediction accuracy. Recently, other variables have been modelled using low density ALS data, such as fuel load (0.5 first returns per m^2) (Gonzalez-Ferreiro et al., 2017), age (0.5–1.5 pulses per m^2) (Maltamo et al., 2020) and berry yields (Bohlin et al., 2021), same dataset as this work) or visibility (30 points per m^2) (Zong et al., 2021a; Zong et al., 2021b), while other studies have focused on predicting combined biomass indices of cervid forage, e.g., Borowik et al. (2013) or species independent abundance (Lone et al. 2014). With regards to this, our study is unique and novel as it aims to separately predict the abundance of low stature trees of six species with great importance as forage for cervids, using an area-based approach.

Our model for abundance of oak had a high predictive power (marginal $R^2 = 0.973$). The Scots pine and birch models had moderately high predictive power (marginal $R^2 = 0.481$ and marginal $R^2 = 0.421$, respectively). For aspen, rowan and willow, marginal R^2 were below 0.4 (0.317, 0.247 and 0.226 respectively), suggesting that these models could not catch variation as successfully as for pine, oak and birch, but still have relatively high R^2 values. One reason for the low explained deviance for some models may be that the abundance of these species is determined by environmental drivers that were not accounted for in our models, like for example soil nutrient availability (De Deyn et al., 2004). Further, our dataset does not discriminate between Sweden's two major *Betula* species (*B. pubescens* and *B. pendula*) which vary in their ecological niches (Maliouchenko et al., 2007). When applying the models to new data, the willow model had the highest rRMSE followed by aspen. High error rates for these two species are not surprising, for two reasons. First, we modelled small scale data on 6.28 m^2 using coarser remote sensing data that cannot be used to identify trees directly, leading us to use an area-based approach. Second, willow and aspen are scarce in our data, and other *Salix* species than *S. caprea* were not included in this dataset. Further, the distribution of willow and aspen also lack a clear geographical trend (compared to oak), which may contribute to the higher rRMSE. In contrast, oak has a distinct southern distribution range in Sweden and climatic variables (here: annual mean temperature and precipitation) accounted for most of the variation in oak abundance, which might explain the comparatively low rRMSE. By including climatic variables in our models, we further facilitate future extrapolation of forage abundance for cervids under given climate change scenarios. This is especially interesting for the oak model, considering that it may expand its distribution northward with increasing temperatures. Such predictions will be of value, not only for understanding cervid forage availability, but also how a changing climate may influence tree regeneration in a broader sense in this region.

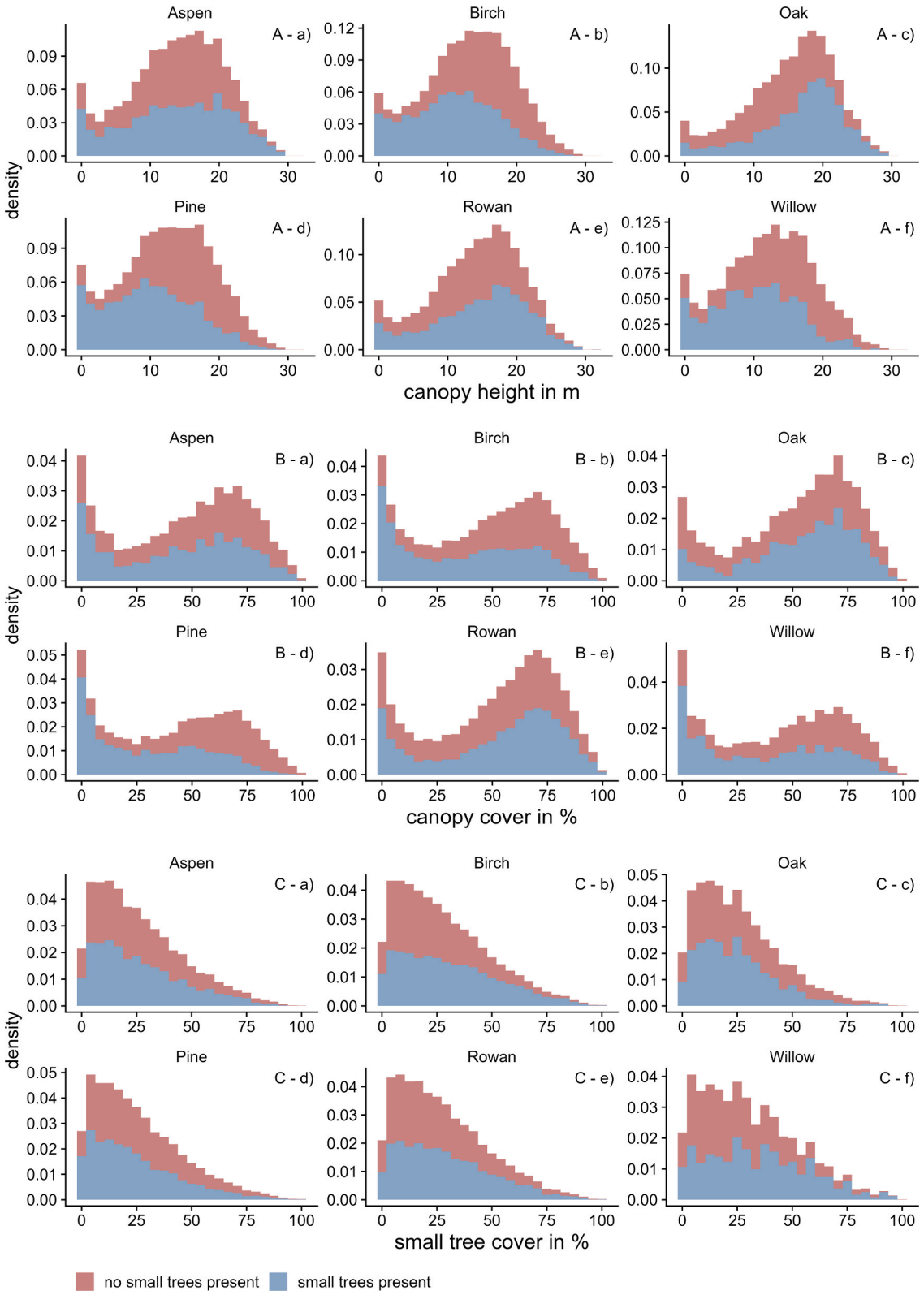

Fig. 4. Density distributions of plots with no small trees (trees within the subplots from 0.1 m height to 4 cm diameter at breast height) (red) and small trees present (blue) across all plots used to train the models (n = 19.461) from the NFI data against three common forest structural metrics based on Airborne Laser Scanning data (canopy height, canopy cover and small tree cover) for all tree species. Panels labeled with capital A show histograms of canopy cover for aspen (*Populus tremula*) (a), birch (*Betulus* spp.) (b), oak (*Quercus* spp.) (c), pine (*Pinus sylvestris*) (d), rowan (*Sorbus aucuparia*) (e) and goat willow (*Salix caprea*) (f). Likewise, panels labelled with B show distributions of canopy cover, and panels labelled with C show the distribution of small tree cover in the data used to train the models. (For interpretation of the references to colour in this figure legend, the reader is referred to the web version of this article.)

4.2. Inclusion of ALS metrics into the models

ALS data has many applications in ecological research (Davies and Asner, 2014; Simonson et al., 2014; Vierling et al., 2008). ALS based metrics ranked amongst the strongest predictors for abundance of most tree species, except for oak, in our study. This highlights that structural forest metrics derived from ALS data provide a suitable data source to model distributions of small trees within the browsing window. Lone et al. (2014) modelled and predicted rowan, oak and willow biomass with correspondingly high accuracy using LiDAR data at a similar low point density, but at a coarser spatial scale (50x50m) than ours (10x10m). One important step forward would be to estimate (tree specific) forage biomass (Johnson et al., 2022) or even to model macronutrient content, as food choice and thus browsing damage may depend on such variables (Felton et al., 2016; Felton et al., 2020).

4.3. Management implications

Holistic and efficient wildlife management needs to consider a wide landscape scale context (Beguin et al., 2016). We provide wall-to-wall remote sensing-based models and spatially explicit maps (Figs. 2–3) that can be used in forest and wildlife management to provide, after testing their usability for management, much needed input for decision making. Within this context, it is important to note that our models or approach to model forage abundance could be applicable, after re-parameterization, in many countries in the boreal zone, and potentially outside of it, to support forest and wildlife management. Further, our modelling approach could be combined with, for example, space-borne LiDAR data and satellite imagery to provide homogenized maps for larger ecoregions or even continents (May et al., 2024; Potapov et al., 2021; Ziegler et al., 2023).

Since 2012, Sweden has an ecosystem-based and adaptive management strategy for moose management. This means that temporal and spatial changes in key factors need to be continuously monitored, and the data should be fed into the management cycle in order for decisions to be adaptive and contributing to reaching set management goals (Bjärstig et al., 2014). Decision makers within Swedish moose management areas (MMA) are currently provided with information from the Swedish Forest Agency regarding the area of young forest within the browsing window (0.5 m–4 m), and a prognosis of how this areal estimate will change in the next few years. Our maps may provide suitable complimentary data for this prognosis, as the maps not only show forage availability across all forest land regardless of forest age or height class, but also because they provide information for each of the six key forage species specifically (AROW, birch, pine). Although novel and tailored towards usage in wildlife management, the suitability of this dataset to inform wildlife management is not given and data should be used with its limitations in mind. Although young forests normally contain higher densities of forage compared to older forests, they often only cover a small fraction of the available landscape for cervids and moose may consume up to 50 % of their tree forage in older forests, further highlighting the importance of considering all forested land in forage estimates (Bergqvist et al., 2018). Which tree species that are available also matters, as some have a stronger influence on mitigating damage on e.g. Scots pine than others (Bergqvist et al., 2014; Felton et al., 2022; Felton et al., 2020; Wallgren et al., 2013; Widén et al., 2024). The next step is to apply our models to see how they improve our understanding of the driving factors behind damage on production trees in Sweden, using national scale monitoring data available for forest management. Further research might also aim to test the models' suitability to help explain variation among moose populations in terms of performance indicators used in regular game monitoring, such as calf body mass and reproduction.

4.4. Outlook

Our models and maps may be directly used in assessments of cervid ecology, for example regarding the spatial variation of cervid space use and browsing damage. For future research, we now have estimates of the amount of available tree forage for cervid species in forest landscapes on a much finer scale than before, which we believe will help disentangle further questions about the roles of alternative forage on browsing damage on Scots pine posed in many studies (Bergqvist et al., 2014; Felton et al., 2022; Felton et al., 2020; Wallgren et al., 2013; Widén et al., 2024). Note however, that for management our maps may be unsuitable for usage at their native resolution (10x10m) for many questions, but instead more suitable if used when aggregated to a 1 ha or 1 km^2 spatial resolution (Figs. 2–3). Further, Lone et al. (2014) showed that their local predictions of forage improved modelling of moose space-use significantly. Therefore, we look forward to the implementation of our high-resolution maps into, for example, future research on the spatiotemporal behavior of moose and other cervids.

To further enhance our understanding of the foodscape for cervids, and how browsing damage on Scots pine occurs within the Fenno-scandian context, we need models of available forage on non-forested land (e.g. mires), e.g. as in Borowik et al. (2013). It is important to note that our maps only consider forested land. Therefore, the landscape level accuracy of forage availability of our maps heavily depends on the proportion of the landscape that is non-forested land. Lastly, in Sweden new national airborne laser scanning data for the same area is collected every 5–10 years. Considering forest growth and disturbances (natural and manmade), we recommend that our maps should be updated with every new round of the Swedish laser scanning survey. With this in mind, it is important to note that Swedish ALS data has a moderately low density (1–2 points per m^2) and an increased point cloud density could help model understory vegetation better.

5. Conclusion

We provide the first national level models and maps of abundance of aspen, birch, oak, Scots pine, rowan and goat willow within the browsing height window, using an extensive dataset from the Swedish National Forest Inventory. These tree species are important in the foraging ecology for many cervid species, especially moose. Therefore, our maps should become a helpful tool to support informed decision making in wildlife management in Sweden. In addition, the models we provide can be applied by forest and wildlife management directly on new data as well. Further, the use of ALS data in the modelling process often revealed strong responses of small tree abundance to the ALS based structural metrics of the first and second order polynomials, as well as their interactions with other variables. This highlights the importance of including the ALS based forest structural metrics into models for small tree abundance. With this in mind, the models we provided in this study showcase an example of how to indirectly model natural resources that cannot be sensed directly through, for example, low density ALS data, but still can provide insights into distributions of forage abundance when modelled appropriately.

CRediT authorship contribution statement

Lukas Graf: Writing – review & editing, Writing – original draft, Visualization, Validation, Software, Methodology, Investigation, Formal analysis, Data curation. **Inka Bohlin:** Writing – original draft, Validation, Supervision, Resources, Project administration, Methodology, Conceptualization. **Per-Ola Hedwall:** Writing – review & editing, Writing – original draft, Visualization, Validation, Supervision, Methodology, Investigation, Funding acquisition, Conceptualization. **Jonas**

Dahlgren: Writing – review & editing, Resources, Project administration, Data curation. **Annika M. Felton:** Writing – review & editing, Writing – original draft, Visualization, Validation, Resources, Project administration, Funding acquisition, Conceptualization.

Declaration of competing interest

The authors declare that they have no known competing financial interests or personal relationships that could have appeared to influence the work reported in this paper.

Acknowledgments

We would like to thank Jonas Jonzen and Mikael Egberth for their support. Further, thanks to Cesko Voeten with his help while fitting the models with the buildmer package. We also thank Ronny Löfstrand and Magnus Hellgren for advice and discussions. We further thank the two anonymous reviewers for the constructive evaluation of our work. The project was funded by Sveaskog and the SLU Forest Damage Centre (SLU.sfak.2022.1.1.1-72-6).

Appendix A. Supplementary data

Supplementary data to this article can be found online at https://doi.org/10.1016/j.jag.2025.104850.

Data availability

We are not allowed to share original data of permanent NFI plots in Sweden. We share data and code for a conceptual reproducible example as well as the model fitting script and data. Both are available from the Zenodo Repository under https://doi.org/10.5281/zenodo.13785127 (Graf et al., 2025).

References

Ågren, A.M., Larson, J., Paul, S.S., Laudon, H., Lidberg, W., 2021. Use of multiple LIDAR-derived digital terrain indices and machine learning for high-resolution national-scale soil moisture mapping of the Swedish forest landscape. Geoderma 404, 115280. https://doi.org/10.1016/j.geoderma.2021.115280.

Apollonio, M., Andersen, R., Putman, R., 2010. European Ungulates and Their Management in the 21st Century. Cambridge University Press, Cambridge.

Apollonio, M., Belkin, V.V., Borkowski, J., Borodin, O.I., Borowik, T., Cagnacci, F., Danilkin, A.A., Danilov, P.I., Faybich, A., Ferretti, F., 2017. Challenges and science-based implications for modern management and conservation of European ungulate populations. Mammal Res. 62, 209–217. https://doi.org/10.1007/s13364-017-0321-5.

Barber, Q.E., Bater, C.W., Braid, A.C., Coops, N.C., Tompalski, P., Nielsen, S.E., 2016. Airborne laser scanning for modelling understory shrub abundance and productivity. For. Ecol. Manage. 377, 46–54. https://doi.org/10.1016/j.foreco.2016.06.037.

Beguin, J., Tremblay, J.P., Thiffault, N., Pothier, D., Côté, S.D., 2016. Management of forest regeneration in boreal and temperate deer–forest systems: challenges, guidelines, and research gaps. Ecosphere 7, e01488. https://doi.org/10.1002/ecs2.1488.

Bergqvist, G., Bergström, R., Wallgren, M., 2014. Recent browsing damage by moose on Scots pine, birch and aspen in young commercial forests–effects of forage availability, moose population density and site productivity. Silva Fenn. 48, 1077. https://doi.org/10.14214/sf.1077.

Bergqvist, G., Wallgren, M., Jernelid, H., Bergström, R., 2018. Forage availability and moose winter browsing in forest landscapes. For. Eco. Manage. 419, 170–178. https://doi.org/10.1016/j.foreco.2018.03.049.

Bjärstig, T., Sandström, C., Lindqvist, S., Kvastegård, E., 2014. Partnerships implementing ecosystem-based moose management in Sweden. Int. J. Biodivers. Sci. Ecosyst. Serv. Manage. 10, 228–239. https://doi.org/10.1080/21513732.2014.936508.

Bohlin, I., Maltamo, M., Hedenås, H., Lämås, T., Dahlgren, J., Mehtätalo, L., 2021. Predicting bilberry and cowberry yields using airborne laser scanning and other auxiliary data combined with National Forest Inventory field plot data. For. Eco. Manage. 502, 119737. https://doi.org/10.1016/j.foreco.2021.119737.

Bohlin, J., Bohlin, I., Jonzén, J., Nilsson, M., 2017. Mapping forest attributes using data from stereophotogrammetry of aerial images and field data from the national forest inventory. Silva Fenn. 51, 2021. https://doi.org/10.14214/sf.2021.

Borowik, T., Pettorelli, N., Sönnichsen, L., Jędrzejewska, B., 2013. Normalized difference vegetation index (NDVI) as a predictor of forage availability for ungulates in forest and field habitats. Eur. K. Wildl. Res. 59, 675–682. https://doi.org/10.1007/s10344-013-0720-0.

Brooks, M.E., Kristensen, K., van Benthem, K.J., Magnusson, A., Berg, C.W., Nielsen, A., Skaug, H.J., Machler, M., Bolker, B.M., 2017. glmmTMB balances speed and flexibility among packages for zero-inflated generalized linear mixed modeling. R J. 9, 378–400. https://doi.org/10.32614/RJ-2017-066.

Côté, S.D., Rooney, T.P., Tremblay, J.-P., Dussault, C., Waller, D.M., 2004. Ecological impacts of deer overabundance. Annu. Rev. Ecol. Evol. Syst. 35, 113–147. https://doi.org/10.1146/annurev.ecolsys.35.021103.105725.

Cukor, J., Vacek, Z., Linda, R., Vacek, S., Marada, P., Šimůnek, V., Havránek, F., 2019. Effects of bark stripping on timber production and structure of Norway spruce forests in relation to climatic factors. Forests 10, 320. https://doi.org/10.3390/f10040320.

Davies, A.B., Asner, G.P., 2014. Advances in animal ecology from 3D-LiDAR ecosystem mapping. Trends Eco. Evol. 29, 681–691. https://doi.org/10.1016/j.tree.2014.10.005.

De Deyn, G.B., Raaijmakers, C.E., van der Putten, W.H., 2004. Plant community development is affected by nutrients and soil biota. J. Ecol. 92, 824–834. https://doi.org/10.1111/j.0022-0477.2004.00924.x.

De Vriendt, L., Barrette, M., Kolstad, A.L., Vuorinen, K., Speed, J.D., Lavoie, S., Tremblay, J.-P., 2023. Heavy browsing pressure by moose (Alces alces) can interfere with the objectives of ecosystem-based forest management. For. Eco. Manage. 549, 121483. https://doi.org/10.1016/j.foreco.2023.121483.

De Vriendt, L., Lavoie, S., Barrette, M., Tremblay, J.P., 2021. From delayed succession to alternative successional trajectory: how different moose browsing pressures contribute to forest dynamics following clear-cutting. J. Veg. Sci. 32, e12945. https://doi.org/10.1111/jvs.12945.

Domisch, T., Huuskonen, S., Matala, J., Nikula, A., 2024. Interactive effects of moose browsing and stand composition on the development of mixed species seedling stands. Silva Fenn. 58, 23077. https://doi.org/10.14214/sf.23077.

Felton, A.M., Felton, A., Raubenheimer, D., Simpson, S.J., Krizsan, S.J., Hedwall, P.O., Stolter, C., 2016. The nutritional balancing act of a large herbivore: an experiment with captive moose (Alces alces L). PLoS One 11, e0150870. https://doi.org/10.1371/journal.pone.0150870.

Felton, A.M., Hedwall, P.-O., Felton, A., Widemo, F., Wallgren, M., Holmström, E., Löfmarck, E., Malmsten, J., Wam, H.K., 2022. Forage availability, supplementary feed and ungulate density: associations with ungulate damage in pine production forests. For. Eco. Manage. 513, 120187. https://doi.org/10.1016/j.foreco.2022.120187.

Felton, A.M., Holmström, E., Malmsten, J., Felton, A., Cromsigt;, J.P., Edenius, L., Ericsson, G., Widemo, F., Wam, H.K., 2020. Varied diets, including broadleaved forage, are important for a large herbivore species inhabiting highly modified landscapes. Sci. Rep. 10, 1904. https://doi.org/10.1038/s41598-020-58673-5.

Fick, S.E., Hijmans, R.J., 2017. WorldClim 2: new 1-km spatial resolution climate surfaces for global land areas. Int. J. Climatol. 37, 4302–4315. https://doi.org/10.1002/joc.5086.

Forbes, E.S., Cushman, J.H., Burkepile, D.E., Young, T.P., Klope, M., Young, H.S., Brody, A., 2019. Synthesizing the effects of large, wild herbivore exclusion on ecosystem function. Funct. Ecol. 33, 1597–1610. https://doi.org/10.1111/1365-2435.13376.

Fridman, J., Holm, S., Nilsson, M., Nilsson, P., Ringvall, A., Ståhl, G., 2014. Adapting national forest inventories to changing requirements – the case of the Swedish national forest inventory at the turn of the 20th century. Silva Fenn. 48 (1095), 10. https://doi.org/10.14214/sf.1095.

Gill, R., 1992. A review of damage by mammals in north temperate forests: 1. Deer. For. Int. J. For. Res. 65, 145–169. https://doi.org/10.1093/forestry/65.2.145.

Gonzalez-Ferreiro, E., Arellano-Perez, S., Castedo-Dorado, F., Hevia, A., Vega, J.A., Vega-Nieva, D., Alvarez-Gonzalez, J.G., Ruiz-Gonzalez, A.D., 2017. Modelling the vertical distribution of canopy fuel load using national forest inventory and low-density airborne laser scanning data. PLoS One 12, e0176114. https://doi.org/10.1371/journal.pone.0176114.

Graf, L., Bohlin, I., Hedwall, P.O., Dahlgren, J., Felton, A., 2025. Data for: Mapping cervid forage in Sweden using remote sensing and national forest inventory data [dataset]. Zenodo. doi: 10.5281/zenodo.13785127.

Herfindal, I., Tremblay, J.-P., Hester, A.J., Lande, U.S., Wam, H.K., 2015. Associational relationships at multiple spatial scales affect forest damage by moose. For. Eco. Manage. 348, 97–107. https://doi.org/10.1016/j.foreco.2015.03.045.

Imangholiloo, M., Saarinen, N., Markelin, L., Rosnell, T., Näsi, R., Hakala, T., Honkavaara, E., Holopainen, M., Hyyppä, J., Vastaranta, M., 2019. Characterizing seedling stands using leaf-off and leaf-on photogrammetric point clouds and hyperspectral imagery acquired from unmanned aerial vehicle. Forests 10, 415. https://doi.org/10.3390/f10050415.

Johnson, L.K., Mahoney, M.J., Bevilacqua, E., Stehman, S.V., Domke, G.M., Beier, C.M., 2022. Fine-resolution landscape-scale biomass mapping using a spatiotemporal patchwork of LiDAR coverages. Int. J. Appl. Earth Obs. Geoinf. 114, 103059. https://doi.org/10.1016/j.jag.2022.103059.

Lantmäteriet, 2020. National Elevation Model, https://www.lantmateriet.se/sv/geodata/vara-produkter/produktlista/markhojdmodell-nedladdning/ (assessed 25 March 2023).

Lantmäteriet, 2022. Laser data Download, forest https://www.lantmateriet.se/sv/geodata/vara-produkter/produktlista/laserdata-nedladdning-skog/ (assessed 25 March 2023).

Lenoir, J., Svenning, J.C., 2014. Climate-related range shifts – a global multidimensional synthesis and new research directions. Ecography 38, 15–28. https://doi.org/10.1111/ecog.00967.

Leys, C., Klein, O., Dominicy, Y., Ley, C., 2018. Detecting multivariate outliers: use a robust variant of the Mahalanobis distance. J. Exp. Soc. Psychol. 74, 150–156. https://doi.org/10.1016/j.jesp.2017.09.011.

Lone, K., van Beest, F.M., Mysterud, A., Gobakken, T., Milner, J.M., Ruud, H.-P., Loe, L. E., 2014. Improving broad scale forage mapping and habitat selection analyses with airborne laser scanning: the case of moose. Ecosphere 5, 144. https://doi.org/10.1890/ES14-00156.1.

Lucas, K.L., Raber, G.T., Carter, G.A., 2010. Estimating vascular plant species richness on Horn Island, Mississippi using small-footprint airborne LIDAR. J. App. Remote Sens. 4, 043545. https://doi.org/10.1117/1.3501119.

Lüdecke, D., Ben-Shachar, M.S., Patil, I., Waggoner, P., Makowski, D., 2021. performance: an R package for assessment, comparison and testing of statistical models. J. Open Source Softw. 6, 3139. https://doi.org/10.21105/joss.03139.

Maliouchenko, O., Palmé, A.E., Buonamici, A., Vendramin, G., Lascoux, M., 2007. Comparative phylogeography and population structure of European Betula species, with particular focus on B. pendula and B. pubescens. J. Biogeogr. 34, 1601–1610. https://doi.org/10.1111/j.1365-2699.2007.01729.x.

Maltamo, M., Kinnunen, H., Kangas, A., Korhonen, L., 2020. Predicting stand age in managed forests using National Forest Inventory field data and airborne laser scanning. For. Ecosyst. 7, 54. https://doi.org/10.1186/s40663-020-00254-z.

Maltamo, M., Næsset, E., Vauhkonen, J., 2014. Forestry Applications of Airborne Laser Scanning. Springer, Dordrecht, Netherlands.

May, P.B., Dubayah, R.O., Bruening, J.M., Gaines, G.C., 2024. Connecting spaceborne lidar with NFI networks: a method for improved estimation of forest structure and biomass. Int. J. Appl. Earth Obs. Geoinf. 129, 103797. https://doi.org/10.1016/j.jag.2024.103797.

Melin, M., Matala, J., Mehtätalo, L., Suvanto, A., Packalen, P., 2016a. Detecting moose (Alces alces) browsing damage in young boreal forests from airborne laser scanning data. Can. J. For. Res. 46, 10–19. https://doi.org/10.1139/cjfr-2015-0326.

Melin, M., Mehtätalo, L., Miettinen, J., Tossavainen, S., Packalen, P., 2016b. Forest structure as a determinant of grouse brood occurrence – an analysis linking LiDAR data with presence/absence field data. For. Eco. Manage. 380, 202–211. https://doi.org/10.1016/j.foreco.2016.09.007.

Mensah, A.A., Jonzén, J., Nyström, K., Wallerman, J., Nilsson, M., 2023. Mapping site index in coniferous forests using bi-temporal airborne laser scanning data and field data from the Swedish national forest inventory. For. Eco. Manage. 547, 121395. https://doi.org/10.1016/j.foreco.2023.121395.

Månsson, J., 2009. Environmental variation and moose Alces alces density as determinants of spatio-temporal heterogeneity in browsing. Ecography 32, 601–612.

Nagelkerke, N.J., 1991. A note on a general definition of the coefficient of determination. Biometrika 78, 691–692. https://doi.org/10.1093/biomet/78.3.691.

Nakagawa, S., Johnson, P.C.D., Schielzeth, H., 2017. The coefficient of determination R^2 and intra-class correlation coefficient from generalized linear mixed-effects models revisited and expanded. J. R. Soc. Interface 14, 20170213. https://doi.org/10.1098/rsif.2017.0213.

Nijland, W., Nielsen, S.E., Coops, N.C., Wulder, M.A., Stenhouse, G.B., 2014. Fine-spatial scale predictions of understory species using climate-and LiDAR-derived terrain and canopy metrics. J. Appl. Remote Sens. 8, 083572. https://doi.org/10.1117/1.JRS.8.083572.

Nikula, A., Matala, J., Hallikainen, V., Pusenius, J., Ihalainen, A., Kukko, T., Korhonen, K.T., 2021. Modelling the effect of moose Alces alces population density and regional forest structure on the amount of damage in forest seedling stands. Pest Manag. Sci. 77, 620–627. https://doi.org/10.1002/ps.6081.

Nilsson, M., Nordkvist, K., Jonzén, J., Lindgren, N., Axensten, P., Wallerman, J., Egberth, M., Larsson, S., Nilsson, L., Eriksson, J., 2017. A nationwide forest attribute map of Sweden predicted using airborne laser scanning data and field data from the National Forest Inventory. Remote Sens. Environ. 194, 447–454. https://doi.org/10.1016/j.rse.2016.10.022.

Pebesma, E.J., 2004. Multivariable geostatistics in S: the gstat package. Comput. Geosci. 30, 683–691. https://doi.org/10.1016/j.cageo.2004.03.012.

Potapov, P., Li, X., Hernandez-Serna, A., Tyukavina, A., Hansen, M.C., Kommareddy, A., Pickens, A., Turubanova, S., Tang, H., Silva, C.E., Armston, J., Dubayah, R., Blair, J. B., Hofton, M., 2021. Mapping global forest canopy height through integration of GEDI and landsat data. Remote Sens. Environ. 253, 112165. https://doi.org/10.1016/j.rse.2020.112165.

R Core Team, 2024. R: A Language and Environment for Statistical Computing. R Foundation for Statistical Computing, 2024. Version 4.4.1, https://www.R-project.org/.

Ripley, B., Venables, B., Bates, D.M., Hornik, K., Gebhardt, A., Firth, D., Ripley, M.B., 2013. Package 'MASS'. CRAN R package, 538, 113–120. doi: 10.32614/CRAN.package.MASS.

Roussel, J.-R., Auty, D., Coops, N.C., Tompalski, P., Goodbody, T.R., Meador, A.S., Bourdon, J.-F., De Boissieu, F., Achim, A., 2020. lidR: an R package for analysis of airborne laser scanning (ALS) data. Remote Sens. Environ. 251, 112061. https://doi.org/10.1016/j.rse.2020.112061.

Simonson, W.D., Allen, H.D., Coomes, D.A., 2014. Applications of airborne lidar for the assessment of animal species diversity. Methods Ecol. Evol. 5, 719–729. https://doi.org/10.1111/2041-210X.12219.

SLU Riksinventering, 2023. Riksinventering av skog. Fältinstruktion 2023. [National forest inventory. Field instructions]. SLU, Institutionen för skoglig resurshushållning, Institutionen för mark och miljö https://www.slu.se/globalassets/ew/org/centrb/rt/dokument/faltinst/ris_fin_2023.pdf (accessed 25 September 2024).

SLU Skogsdata, 2019. Sveriges officiella statistic. [Forest data. Swedish official statistic]. SLU, Institutionen för skoglig resurshushållning, (accessed 25 March 2023).

Spitzer, R., 2019. Trophic resource use and partitioning in multispecies ungulate communities. Acta. Univ. Agric. Suec. 73, 121.

Swedish Forest Agency, 2024. Älgbetesinventeringen och Foderprognos. 2024. https://www.skogsstyrelsen.se/statistik/statistik-efter-amne/abin-och-foderprognos (accessed 25 March 2025).

Swedish Land Survey, 2020. Digital data maps of land cover, elevation and infrastructure. 2020. http://www.lantmateriet.se (accessed 25 March 2025).

Tomppo, E., Gschwantner, T., Lawrence, M., McRoberts, R.E., Gabler, K., Schadauer, K., Vidal, C., Lanz, A., Ståhl, G., Cienciala, E., 2010. National forest inventories: Pathways for Common Reporting. Springer, Dordrecht.

Vierling, K.T., Vierling, L.A., Gould, W.A., Martinuzzi, S., Clawges, R.M., 2008. Lidar: shedding new light on habitat characterization and modeling. Front. Ecol. Environ. 6, 90–98. https://doi.org/10.1890/070001.

Voeten, C.C., 2021. Package 'buildmer'. Cran R 10.32614/CRAN.package.buildmer.

Walck, J.L., Hidayati, S.N., Dixon, K.W., Thompson, K., Poschlod, P., 2011. Climate change and plant regeneration from seed. Glob. Chang. Biol. 17, 2145–2161. https://doi.org/10.1111/j.1365-2486.2010.02368.x.

Wadoux, A.M.J.C., Heuvelink, G.B.M., 2023. Uncertainty of spatial averages and totals of natural resource maps. Methods Ecol. Evol. 14, 1320–1332. https://doi.org/10.1111/2041-210x.14106.

Wallgren, M., Bergström, R., Bergqvist, G., Olsson, M., 2013. Spatial distribution of browsing and tree damage by moose in young pine forests, with implications for the forest industry. For. Eco. Manage. 305, 229–238. https://doi.org/10.1016/j.foreco.2013.05.057.

Wam, H.K., Hofstad, O., 2007. Taking timber browsing damage into account: a density dependant matrix model for the optimal harvest of moose in Scandinavia. Ecol. Econ. 62, 45–55. https://doi.org/10.1016/j.ecolecon.2007.01.001.

Widén, A., Felton, A.M., Widemo, F., Singh, N.J., Cromsigt;, J.P., 2024. Deer in the agriculture-forest matrix: interacting effects of land uses on browsing pressure on trees. For. Eco. Manage. 563, 121890. https://doi.org/10.1016/j.foreco.2024.121890.

Widén, A., Jarnemo, A., Månsson, J., Lilja, J., Morel, J., Felton, A.M., 2022. Nutrient balancing or spring flush–what determines spruce bark stripping level by red deer? For. Eco. Manage. 520, 120414. https://doi.org/10.1016/j.foreco.2022.120414.

Ziegler, A., Heisig, J., Ludwig, M., Reudenbach, C., Meyer, H., Nauss, T., 2023. Using GEDI as training data for an ongoing mapping of landscape-scale dynamics of the plant area index. Environ. Res. Lett. 18, 075003. https://doi.org/10.1088/1748-9326/acde8f.

Zong, X., Wang, T., Skidmore, A.K., Heurich, M., 2021a. Estimating fine-scale visibility in a temperate forest landscape using airborne laser scanning. Int. J. Appl. Earth Obs. Geoinf. 103, 102478. https://doi.org/10.1016/j.jag.2021.102478.

Zong, X., Wang, T., Skidmore, A.K., Heurich, M., 2021b. The impact of voxel size, forest type, and understory cover on visibility estimation in forests using terrestrial laser scanning. Gisci. Remote Sens. 58, 323–339.